Selective killing of oncogenically transformed cells through a ROS-mediated mechanism by β-phenylethyl isothiocyanate

Dunyaporn Trachootham,[1,2,3] Yan Zhou,[1] Hui Zhang,[1,2] Yusuke Demizu,[1] Zhao Chen,[1,2] Helene Pelicano,[1] Paul J. Chiao,[2,4] Geetha Achanta,[1] Ralph B. Arlinghaus,[1,2] Jinsong Liu,[2,5] and Peng Huang[1,2,*]

[1] Department of Molecular Pathology, The University of Texas M.D. Anderson Cancer Center, Houston, Texas 77030
[2] The University of Texas Graduate School of Biomedical Sciences at Houston, Houston, Texas 77030
[3] Faculty of Dentistry, Thammasat University, Rangsit Campus, Pathum-thani, Thailand 12121
[4] Department of Surgical Oncology, The University of Texas M.D. Anderson Cancer Center, Houston, Texas 77030
[5] Department of Pathology, The University of Texas M.D. Anderson Cancer Center, Houston, Texas 77030
*Correspondence: phuang@mdanderson.org

Summary

Reactive oxygen species (ROS) stimulate cell proliferation and induce genetic instability, and their increase in cancer cells is often viewed as an adverse event. Here, we show that such abnormal increases in ROS can be exploited to selectively kill cancer cells using β-phenylethyl isothiocyanate (PEITC). Oncogenic transformation of ovarian epithelial cells with *H-Ras*^{V12} or expression of *Bcr-Abl* in hematopoietic cells causes elevated ROS generation and renders the malignant cells highly sensitive to PEITC, which effectively disables the glutathione antioxidant system and causes severe ROS accumulation preferentially in the transformed cells due to their active ROS output. Excessive ROS causes oxidative mitochondrial damage, inactivation of redox-sensitive molecules, and massive cell death. In vivo, PEITC exhibits therapeutic activity and prolongs animal survival.

Introduction

Therapeutic selectivity is an important issue in cancer treatment. An ideal anticancer agent should be toxic to malignant cells with minimum toxicity in normal cells. However, currently there are limited numbers of such agents available for clinical use. Thus, development of novel selective drugs is an important and challenging task, and understanding the biological differences between normal and cancer cells is essential for achieving this goal. A prime example of successful design of selective anticancer drugs is the development of Gleevec, which targets the oncogenic tyrosine kinase BCR-ABL responsible for human chronic myeloid leukemia (Ren, 2005). While identifying specific oncogenes responsible for cancer development and designing targeting agents represent a very important research area, such tasks have proven to be challenging, due to multiple genetic and epigenetic alterations in cancer cells (Couzin, 2002; Frantz, 2005). Mutations or overexpression of the target molecules often lead to drug resistance and impose further challenge in treatment of cancer using such target-specific agents. This situation has prompted the consideration of alternative approaches. Instead of targeting specific oncogenic molecules, it may be possible to exploit the biochemical alterations in cancer cells as a basis for developing selective therapeutic agents. If a biochemical alteration is common in cancer cells, targeting such change would have broad therapeutic applications.

One common biochemical change in cancer cells is the increase in reactive oxygen species (ROS) generation. Emerging evidences suggest that most cancer cells are under oxidative stress associated with increased metabolic activity and production of ROS (Szatrowski and Nathan, 1991), although in some cases the observed ROS increase could be due to sample handling and analytical artifacts (Swartz and Gutierrez, 1977). The ROS increase is thought to play an important role in maintaining cancer phenotype due to their stimulating effects on cell growth and proliferation (Hu et al., 2005), genetic instability (Radisky et al., 2005), and senescence evasion (Chen et al., 2005). Owing to their cancer-promoting effect, increased ROS in cancer cells is often considered as an adverse factor. However, high levels of ROS can also cause cellular damage, depending on the levels and duration of ROS stress (Pelicano et al., 2004). These dose- and time-dependent effects may provide an opportunity

SIGNIFICANCE

Most cancer cells exhibit elevated ROS generation associated with active metabolism and oncogenic stimulation. Although this phenomenon has long been recognized, its therapeutic implications remain unclear. The current study demonstrated that it is possible to take advantage of this ROS stress in cancer and use ROS-mediated mechanisms to preferentially kill the malignant cells. This therapeutic strategy can be achieved both in vitro and in vivo, using a natural compound, PEITC. Thus, ROS stress associated with oncogenic transformation may serve as a biochemical basis for developing cancer therapeutics. Furthermore, because PEITC has low toxicity in nonmalignant cells and exhibits anticancer selectivity superior to cisplatin, it is a promising compound and potentially has significant therapeutic applications.

to exploit the cell killing potential of ROS by using exogenous ROS-stressing agents to increase the intracellular ROS to a toxic level, or the threshold that triggers cell death. For instance, human leukemia cells with intrinsic oxidative stress are highly sensitive to ROS stress induced by 2-methoxyestradiol and arsenic trioxide (Huang et al., 2000; Zhou et al., 2003). Promoting ROS generation in mitochondria was shown to effectively kill cancer cells (Pelicano et al., 2003). Although induction of ROS generation by anticancer drugs including doxorubicin, arsenic trioxide, and taxol has been observed, it is still unclear whether the intrinsic oxidative stress in cancer cells could provide a selective response to ROS-generating agents.

Because increased ROS generation is common in cancer cells with active metabolism under the influence of oncogenic signals including *Ras*, *Bcr-Abl*, and *c-Myc* (Irani et al., 1997; Sattler et al., 2000; Vafa et al., 2002), we postulated that the intrinsic ROS stress associated with oncogenic transformation would make the cells highly dependent on their antioxidant systems to counteract the damaging effect of ROS and to maintain redox balance in a dynamic state (increased ROS generation and active ROS scavenging). This situation would render them highly vulnerable to further oxidative insults by exogenous agents. On the other hand, normal cells may better tolerate such an intervention owing to their low basal ROS output and normal metabolic regulation. As such, the differences in redox states between normal and cancer cells may provide a biological basis for selective killing of malignant cells, using agents that cause further ROS stress.

β-phenylethyl isothiocyanate (PEITC) is a natural compound found in consumable cruciferous vegetables with chemopreventive activity (Yu et al., 1998). Recent studies suggest that, in contrast to the view of PEITC as an antioxidant, this compound could increase ROS generation and induce apoptosis in cancer cell lines (Yu et al., 1998; Zhang et al., 2003; Wu et al., 2005). However, whether PEITC has a selective effect against cancer cells and whether the intrinsic redox status could affect the fate of cellular response to ROS-modulating agents remain unclear. The goal of this study was to test the concept that increased ROS generation associated with oncogenic transformation may serve as a biochemical basis to selectively kill cancer cells using redox-modulating agents.

Results

Oncogenic transformation by *H-Ras* or *Bcr-Abl* leads to increased ROS generation

To test the hypothesis that oncogenic transformation causes increased ROS generation and renders the transformed cells vulnerable to further ROS stress, we first used in vitro systems to evaluate the effects of two oncogenic signals, *Ras* and *Bcr-Abl*, on ROS generation and cellular sensitivity to exogenous ROS stress under isogenic conditions. A previously immortalized normal ovarian epithelial cell line (T72 cells harboring *SV-40 T/t* and *hTERT*) was further transfected with *H-Ras*^{V12} (Liu et al., 2004). The stably transfected cells (T72Ras) exhibited malignant behaviors capable of forming foci in soft agar and growing tumor in vivo. As illustrated in Figure 1A, T72Ras cells readily formed tumor in all 20 mice tested and exhibited pathological morphology resembling human ovarian clear cell carcinoma. Western blot analysis showed that T72Ras cells expressed increased H-RAS, which was functionally active, as evidenced

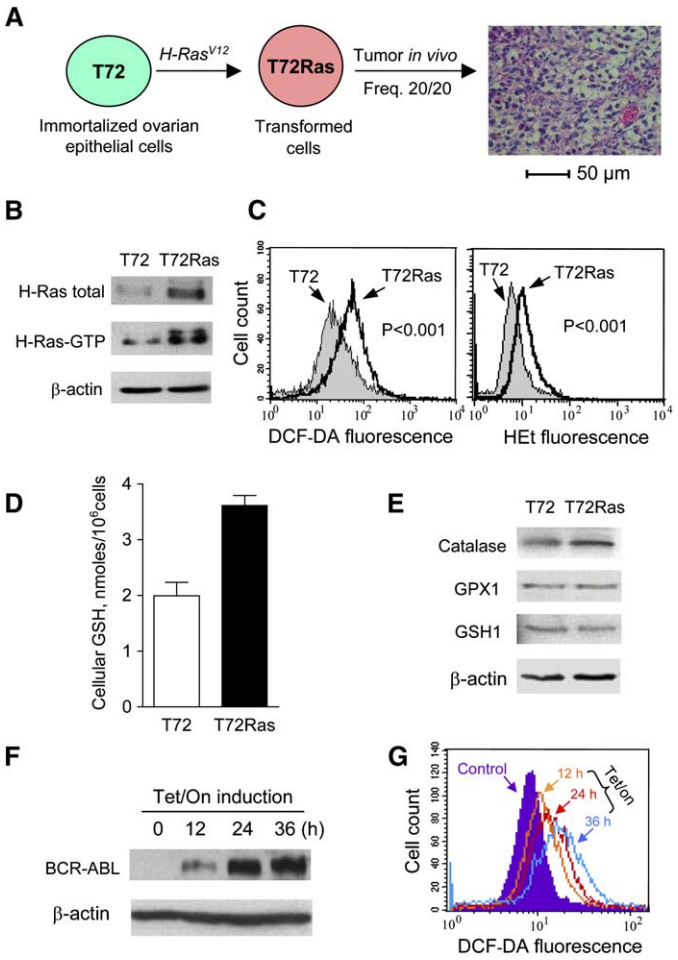

Figure 1. Oncogenic transformation by *H-Ras* or *Bcr-Abl* causes increased ROS generation

A: T72Ras cells derived from T72 cells by *Ras* transformation readily formed tumors in all 20 mice tested. Tumor tissue stained with hematoxylin-eosin exhibited pathological morphology resembling human ovarian clear cell carcinoma.

B: Basal H-RAS protein expression and RAS activation in T72Ras cells, measured by Western blot and immunoprecipitation assays.

C: Increase of ROS in T72Ras cells detected by flow cytometry using DCF-DA (left panel) and HEt (right panel). Each histogram is representative of three experiments ($p < 0.001$, T72 versus T72Ras cells).

D: Comparison of total cellular GSH in T72 and T72Ras cells (mean ± SD of three experiments; $p < 0.05$).

E: Basal protein expression of catalase, glutathione peroxidase 1 (GPX1), and γ glutamyl-cysteine synthetase enzyme (GSH1) in T72 and T72Ras cells.

F: Time-dependent induction of BCR-ABL expression by doxycycline (1 μg/ml) in TonB210 cells.

G: Increase of ROS in TonB210 cells after induction of BCR-ABL expression.

by constitutive RAS-GTP activity (Figure 1B). Importantly, compared to the parental T72 cells, the *Ras*-transformed cells exhibited a significant increase (200%) in basal ROS content, as quantified by flow cytometry using CM-H_2DCF-DA as a fluorescent probe (Figure 1C, fluorescence in log-scale). We also used hydroethidine (HEt), a relatively specific probe for superoxide (O_2^-) (Zhao et al., 2003), to compare the basal levels of O_2^- in the two cell lines. T72Ras cells exhibited significantly higher HEt fluorescence (11 units) than T72 cells (6 units; $p < 0.001$), suggesting an increase in basal O_2^- in the *Ras*-transformed cells (Figure 1C, right panel). Further analyses revealed that

the elevated ROS was not due to a decrease in antioxidant capacity, since there was a significant increase in cellular glutathione (GSH) and an upregulation of catalase (Figures 1D and 1E). There was no change in expression of glutathione peroxidase (GPX-1) and γ-glutamyl-cysteine synthetase (GSH1). These data together suggest that transformation of ovarian epithelial cells with *H-Ras* led to increased ROS generation and a compensatory increase in cellular antioxidant activity.

A stable clone of murine hematopoietic cells harboring a tetracycline-inducible *Bcr-Abl* expression vector (TonB210 cells; Klucher et al., 1998) was then used to test if induced expression of *BCR-ABL* would also cause increased ROS generation. As illustrated in Figure 1F, addition of doxycycline induced BCR-ABL expression and a time-dependent increase in cellular ROS detected by DCF-DA (Figure 1G). In control experiments, doxycycline incubation under the same conditions did not cause an increase of DCF-DA fluorescence in the parental cells (data not shown), suggesting that the ROS increase in TonB210 cells was due to BCR-ABL expression.

Increased ROS generation renders the oncogenically transformed cells highly sensitive to PEITC

Evaluation of cellular response to ROS-modulating agents revealed a striking preferential activity of PEITC against the transformed cells. Treatment of T72Ras cells with 10 μM PEITC caused a substantial increase in DCF-DA-reactive ROS in a time-dependent manner and reached a 16-fold increase at 5 hr (Figure 2A). In contrast, the parental T72 cells were less sensitive to PEITC, showing a moderate ROS elevation without further increase as the incubation prolonged (Figure 2B), suggesting that the nonmalignant cells could better cope with PEITC-induced ROS accumulation, likely due to their low basal ROS output (Figure 1C). Quantitative analysis further confirmed the significant difference between T72Ras and T72 cells in ROS induction by 5 μM PEITC for various times (Figure 2C). This difference also held true when both cell lines were exposed to various concentrations of PEITC (Figure S1 in the Supplemental Data available with this article online). Interestingly, there was no significant change in HEt fluorescence after treatment with PEITC in either cell line, although the *Ras*-transformed cells consistently exhibited a higher basal O_2^- (Figure S2A), suggesting that ROS induced by PEITC were mainly DCF-DA-reactive species such as hydrogen peroxide (H_2O_2) and nitric oxide (NO), but not O_2^-. Using 4-amino-5-methylamino-2′,7′-difluorofluorescein (DAF-FM), a relatively specific probe for NO (Balcerczyk et al., 2005), we showed that treatment of T72Ras cells with 5 μM PEITC significantly increased DAF-FM fluorescence, which was reversed by the antioxidant *N*-acetyl-*L*-cysteine (NAC) but not by the H_2O_2-scavenging enzyme catalase (Figure S2B). In contrast, the PEITC-induced increase in DCF-DA fluorescence could be readily reversed by either NAC or catalase.

The significant difference between T72 and T72Ras cells in their ROS accumulation in response to PEITC prompted us to compare the cytotoxic effect of this compound in the two cell lines. Flow cytometric analysis showed that PEITC effectively induced cell death in T72Ras cells in a time-dependent manner, causing approximately 50% cell death in 5 hr (Figure 2D). In contrast, T72 cells were significantly less sensitive to PEITC at all time points tested (Figure 2D). The preferential killing of *Ras*-transformed cells by PEITC was further demonstrated with multiple drug concentrations (Figure 2E) and various times

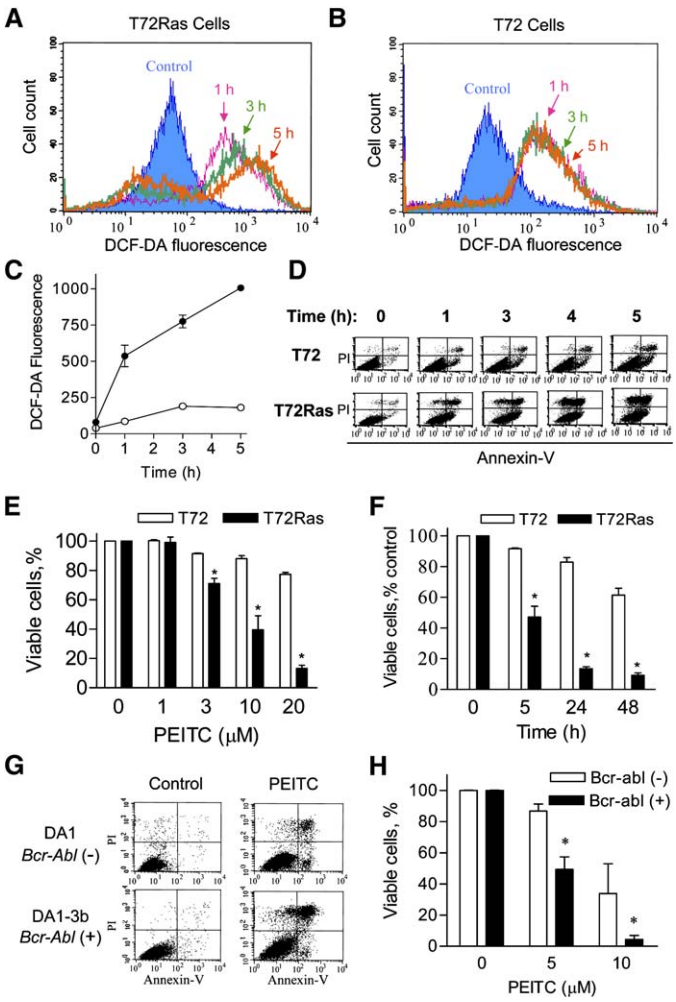

Figure 2. Preferential induction of ROS accumulation and cell death by PEITC in oncogenically transformed cells

A: Time-dependent ROS accumulation induced by 10 μM PEITC in T72Ras cells. ROS were measured by flow cytometry using DCF-DA.

B: Effect of PEITC (10 μM) on cellular ROS content in T72 cells.

C: Comparison of ROS in T72Ras cells (black circles) and T72 cells (white circles) induced by 5 μM PEITC (mean ± SD of three experiments).

D: Time-dependent cell death induced by 10 μM PEITC in T72Ras and T72 cells. Cell death was measured by annexin-V/PI assay. The dot plots are representative of three experiments.

E: Dose-dependent killing by PEITC (5 hr) in T72Ras and T72 cells (mean ± SD of three experiments; *$p < 0.05$).

F: Time-dependent killing of T72Ras and T72 cells by 10 μM PEITC (mean ± SD from three experiments; *$p < 0.05$).

G: Comparison of PEITC-induced cell death (5 μM, 24 hr) in *Bcr-Abl* transformed cells (DA1-3b) and the parental DA1 cells.

H: Dose-dependent killing by PEITC (24 hr) in DA1-3b cells and DA1 cells (mean ± SD of three experiments; *$p < 0.05$).

(Figure 2F). Similarly, the highly aggressive mouse leukemia cells (DA1-3b) constitutively expressing BCR-ABL were more sensitive to PEITC than the parental cells (DA1, myeloid progenitor cells). As shown in Figure 2G, incubation of DA1-3b cells with 5 μM PEITC resulted in 50% cell death but only caused 10% cell death in DA1. This differential sensitivity was also observed at 10 μM of PEITC (Figure 2H) and with various incubation times (Figure S3).

Because the nonmalignant T72 cells could not form colonies, we adapted the MTT assay to compare PEITC's effect

on long-term cell proliferation in T72 and T72Ras cells. As shown in Figure 3A, this compound exhibited greater inhibition on T72Ras cells during 10 day incubation. We then compared this selectivity with cisplatin (CDDP), a common drug for ovarian cancer treatment. Both the long-term cell proliferation assay (10 day MTT; Figure 3B) and acute cell death analysis by annexin-V/PI staining (Figure 3C) showed that CDDP exerted a similar effect on T72 and T72Ras cells. The ratio of IC_{50} values for T72 cells and T72Ras cells was 1.0 for CDDP and 3.9 for PEITC (Figure 3D), suggesting that PEITC has a better selectivity. Since CDDP was shown to increase ROS in certain cells, we compared the ROS levels before and after CDDP exposure. As shown in Figure 3E, in both T72 and T72Ras cells, CDDP caused no change in ROS after 4 hr incubation and only a slight increase in DCF-DA fluorescence after 24 hr. These observations suggest that the cytotoxic effect of CDDP in these cells was unlikely triggered by ROS.

ROS-mediated damage is a critical mechanism for PEITC-induced cell death

The above observations suggest that ROS might mediate the anticancer activity of PEITC. To further test if PEITC could preferentially induce ROS-mediated lipid peroxidation in *Ras*-transformed cells, we treated T72 and T72Ras cells with 10 μM PEITC for various times and used nonyl acridine orange (NAO) to detect oxidation of cardiolipin, a mitochondrial membrane lipid component (Nomura et al., 2000). As shown in Figure 4A, PEITC caused a massive cardiolipin oxidation in the T72Ras cells, evidenced by a time-dependent left shift of NAO fluorescence. About 50% and 88% of T72Ras cells lost their cardiolipin within 4 hr and 8 hr, respectively. Addition of antioxidant NAC almost completely reversed the PEITC-induced loss of NAO staining (Figure 4A, right panel), suggesting that the decrease of NAO fluorescence was due to oxidative damage. In contrast, only a small percent of T72 cells showed a loss of NAO signal (Figure 4A).

A second assay was used to confirm the preferential induction of mitochondrial membrane damage by PEITC. The functional integrity of mitochondrial membranes was assessed by flow cytometry after cells were labeled with rhodamine-123 (Rho-123), a potential-sensitive dye that accumulates in intact mitochondria and emits red fluorescence. A decrease of this fluorescence indicates a loss of transmembrane potential (Sureda et al., 1997). As shown in Figure 4B, PEITC caused a time-dependent loss of Rho-123 signal in T72Ras cells starting at 4 hr, and 64% of cells lost their mitochondrial integrity by 8 hr. In contrast, only a small portion of the nontransformed cells exhibited a loss of Rho-123 signal. Interestingly, when the time courses for cardiolipin oxidation (Figure 4A) and loss of transmembrane potential (Figure 4B) in T72Ras cells were compared, it appeared that membrane oxidation occurred first, followed by the loss of membrane integrity with a delay of approximately 1–2 hr.

The relationship between ROS accumulation and PEITC-induced cell death was evaluated quantitatively by plotting the percent of cell death as a function of ROS increase (Figure 4C). There was a strong correlation between these two parameters ($r = 0.9727$; $p < 0.001$). To verify the cause-effect relationship between ROS increase and cell death, we tested the effect of H_2O_2-scavenging enzyme catalase on PEITC-induced cell death in T72Ras cells. Since H_2O_2 is relatively stable and can diffuse across cellular membranes, addition of catalase to the cell culture could reduce cellular H_2O_2 due to its dynamic balance across the

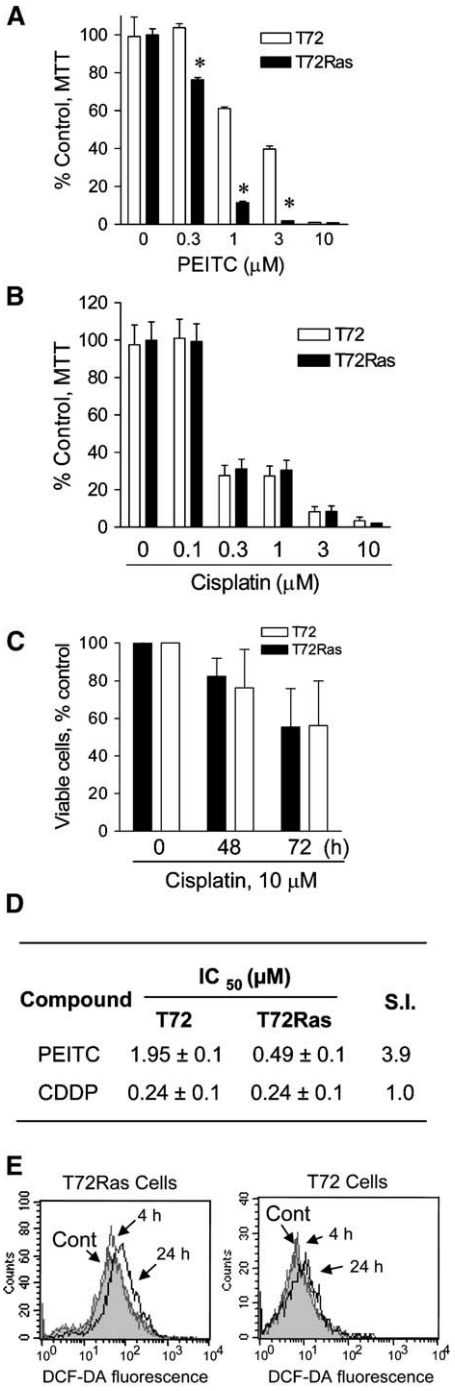

Compound	IC 50 (μM)		S.I.
	T72	T72Ras	
PEITC	1.95 ± 0.1	0.49 ± 0.1	3.9
CDDP	0.24 ± 0.1	0.24 ± 0.1	1.0

Figure 3. Anticancer selectivity of PEITC is superior to that of cisplatin in vitro

A: Inhibition of cell proliferation by PEITC in T72 and T27Ras cells. Cell growth inhibition was measured by long-term MTT assay (mean ± SD of three experiments; *$p < 0.05$).

B: Dose-dependent inhibition of cell proliferation by cisplatin in T72Ras and T72 cells, measured by long-term MTT assay (mean ± SD of three experiments).

C: Cytotoxicity of cisplatin (10 μM) in T72Ras and T72 cells measured by annexin-V/PI assay (mean ± SD of three experiments).

D: Comparison of in vitro selectivity of PEITC and cisplatin (CDDP). The concentrations required to inhibit 50% cell proliferation (IC_{50}) were determined using the 10 day MTT assay, and the selectivity index (S.I.) was calculated as the IC_{50} ratio of T72/T72Ras cells.

E: Effect of CDDP (10 μM) on cellular ROS in T72Ras and T72 cells.

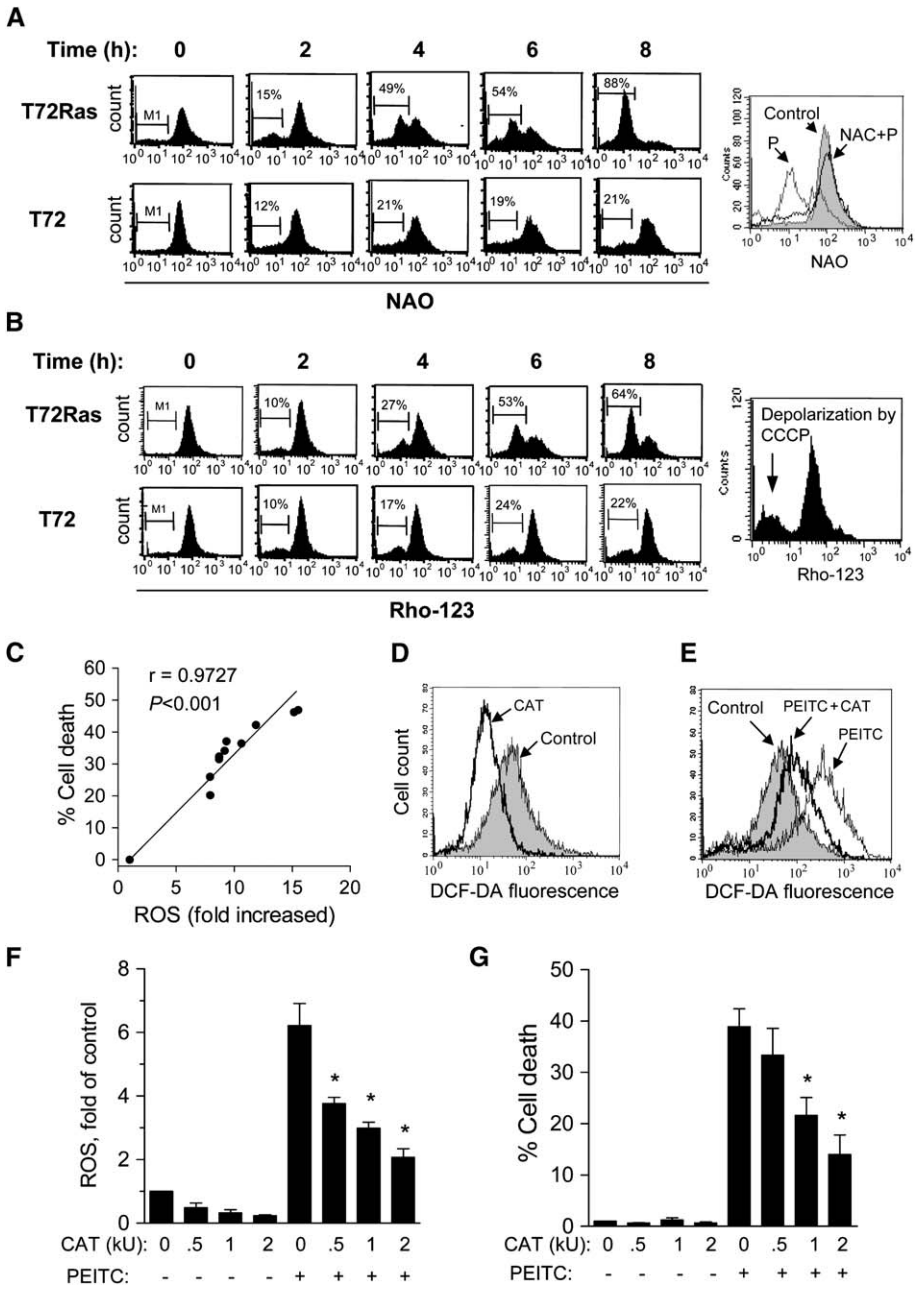

Figure 4. Selective killing of *Ras*-transformed cells by PEITC through ROS-mediated damage

A: Comparison of oxidative damage to cardiolipin by 10 μM PEITC in T72 and T72Ras cells measured by flow cytometry using NAO. M1 indicates subpopulation of cells that lost NAO signal due to cardiolipin oxidation. The right panel shows that NAC (1 mM) reversed the loss of NAO signal in T72Ras cells treated with PEITC (10 μM, 6 hr).

B: Preferential induction of mitochondrial transmembrane potential loss by 10 μM PEITC in T72Ras cells detected by flow cytometry using Rho-123. M1 indicates subpopulation of cells that lost transmembrane potential. The right panel shows the effect of the uncoupling agent CCCP (100 μM) as a positive control for membrane potential collapse.

C: Correlation between ROS increase and PEITC-induced cell death in T72Ras cells. ROS and cell death were measured by DCF-DA and annexin-V/PI assays, respectively. Data points from three experiments using 10 μM PEITC for various times were analyzed by linear regression.

D: Effect of exogenous catalase (CAT, 2000 U/ml, 6 hr) on the basal ROS level in T72Ras cells.

E: Reversion of PEITC-induced ROS accumulation by catalase. T72Ras cells were pretreated with catalase (2000 U/ml, 1 hr), followed by 5 μM PEITC for 5 hr.

F: Effects of catalase (0-2000 U/ml, preincubation for 1 hr) and PEITC (5 μM, 5 hr) on ROS levels in T72Ras cells detected by DCF-DA (mean ± SD of three experiments; *p < 0.05).

G: Effect of catalase on PEITC-induced cell death. T72Ras cells were pretreated with catalase for 1 hr, followed by 5 μM PEITC for 5 hr. Cell death was detected by annexin-V/PI assay (mean ± SD of three experiments; *p < 0.05).

membranes. Indeed, exogenous catalase decreased the basal ROS in T72Ras cells (Figure 4D) and significantly offset the ROS increase induced by PEITC (Figure 4E). Quantitative analysis showed that catalase significantly reduced PEITC-induced ROS accumulation in a dose-dependent manner (Figure 4F) and proportionally abrogated PEITC-induced cell death (Figure 4G), suggesting that H_2O_2 was critical in mediating cytotoxicity.

We further tested if PEITC could cause cytochrome c release from mitochondria and activate caspases. PEITC (5–10 μM) caused a rapid release of cytochrome c from mitochondria to cytosol within 5 hr in T72Ras cells, but this did not result in a significant activation of caspase-3 (Figure S4). This is consistent with oxidation of caspase-3 by ROS, a process known to abrogate caspase activation (Hampton et al., 2002). Thus, it appeared that PEITC caused a severe damage to mitochondria membranes and cytochrome c release, but the increased ROS prevented caspase activation, leading to necrotic cell death. This was consistent with the cell death profiles revealed by annexin-V/PI staining showing a large population of necrotic cells in the up-left quarter of the flow cytometry plots (Figure 2D; T72Ras cells). Interestingly, cells overexpressing Bcl-2, a molecule with antioxidant function capable of protecting the mitochondrial integrity (Hockenbery et al., 1993), were less sensitive to PEITC (Figure S5), suggesting the important role of mitochondrial damage in PEITC-induced cell death.

PEITC causes severe ROS accumulation in *Ras*-transformed cells by disabling the GSH antioxidant system

Since PEITC exerted cytotoxicity by causing excessive ROS accumulation, we then investigated the mechanisms by which PEITC caused ROS increase. Based on the important role of

GSH as a major cellular antioxidant and the observation that PEITC can conjugate with GSH for export from leukemia cells (Xu and Thornalley, 2001), we postulated that the active ROS generation in *Ras*-transformed cells would render them highly dependent on GSH to maintain redox balance, and that a depletion of GSH by PEITC would result in an excessive accumulation of ROS to a threshold that triggers cell death. To test this possibility, we first examined the effect of PEITC on GSH contents. As shown in Figure 5A, incubation of T72Ras cells with 5 μM PEITC led to a depletion of cellular GSH by 75% in 1 hr, and almost complete depletion in 3 hr. In T72 cells treated with 5 μM PEITC, approximately 40% and 20% GSH remained at 1 and 3 hr, respectively. Analysis of GSH in the medium showed that GSH was rapidly exported from the cells (Figure 5B). The amount of GSH in the medium was quantitatively accountable for the GSH loss in the cells (calculated based on cell number and volume), suggesting that PEITC-induced GSH export was a key mechanism for GSH depletion. Interestingly, catalase effectively abolished PEITC-induced ROS increase (Figure 5C) but did not prevent GSH depletion (Figure 5D), suggesting that the depletion of GSH was not secondary to ROS stress.

In contrast, pretreatment of T72Ras cells with 3 mM NAC, a precursor of GSH and a potent antioxidant (Deneke, 2000), effectively prevented PEITC-induced GSH depletion (Figure 5E) and ROS accumulation (Figure 5F). Importantly, NAC also suppressed the cytotoxicity of PEITC (Figure 5G), suggesting that depletion of cellular GSH is an important mechanism responsible for PEITC-induced ROS accumulation and cell death. To further demonstrate the important role of GSH in the survival of *Ras*-transformed cells, we used buthionine sulfoximine (BSO), an inhibitor of GSH synthesis, to test if this agent could also cause preferential killing of the *Ras*-transformed cells. We showed that BSO indeed exhibited greater cytotoxic effect on T72Ras cells compared to T72 cells, although a longer incubation (24 hr) and higher concentrations were required to achieve significant cell killing (Figure S6).

Because GPX is the major enzyme that uses GSH as the substrate to scavenge peroxides, we tested if PEITC might affect GPX activity and compromise the cell's ability to use the remaining GSH. Incubation of purified human GPX with PEITC in vitro resulted in a concentration-dependent inhibition of GPX activity (Figure 6A). In the cell-free enzyme assay, 100 and 500 μM PEITC inhibited GPX by approximately 50% and 90%, respectively. These concentrations could be achieved intracellularly when cells were incubated with 5–10 μM PEITC. HPLC analysis showed that incubation of T72Ras cells with 5 and 10 μM PEITC for 2 hr resulted in an accumulation of intracellular PEITC of 252 and 590 μM, respectively (Figure S7). Analysis of GPX activity in protein extracts from cells pretreated with 10 μM PEITC exhibited a significant reduction in GPX enzyme activity (Figure 6B) without a loss of GPX protein (Figure 6C). These data suggest that PEITC not only depletes cellular GSH pool but can also inhibit GPX enzyme as dual mechanisms to disable the GSH antioxidant system, leading to severe ROS accumulation in malignant cells that are active in ROS generation.

Interestingly, we also found that PEITC significantly abolished the H-RAS-GTP activity, as demonstrated in a pulldown assay showing an almost complete loss of H-RAS binding with RAF-1 after cells were incubated with 5 μM PEITC for 3 hr (Figure 6D). This loss of H-RAS-GTP activity was not due to a decrease of H-RAS protein (Figure 6D, middle panel). The antioxidant NAC

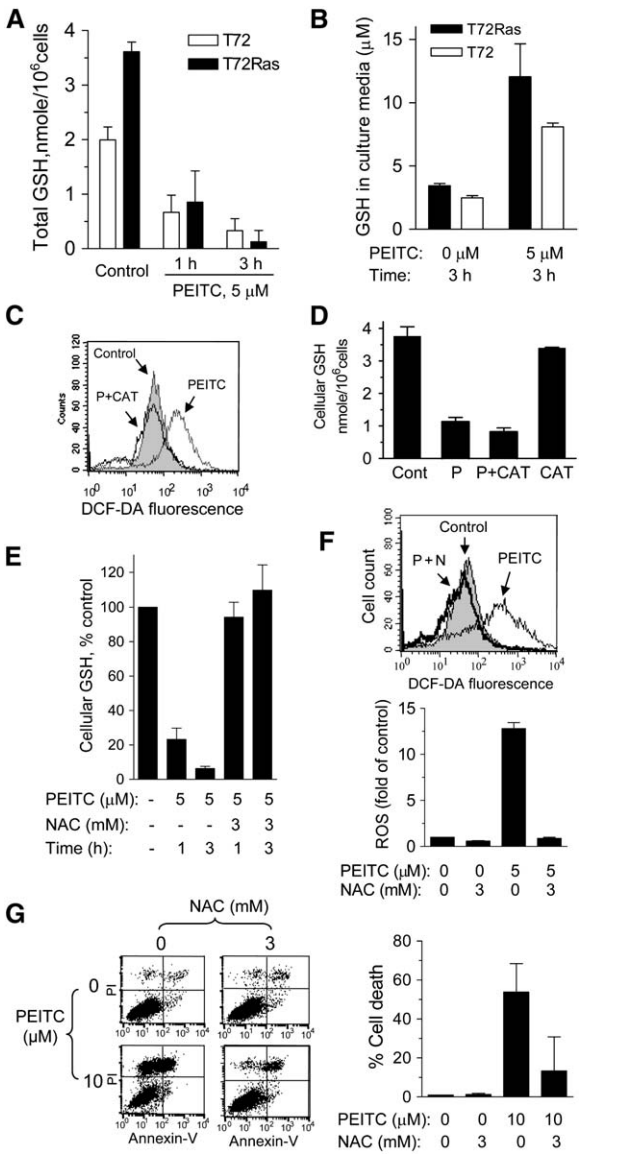

Figure 5. PEITC causes depletion of cellular GSH and its reversion by NAC

A: Time-dependent depletion of GSH by PEITC (5 μM, 1–3 hr) in T72 and T72Ras cells. Cellular GSH was measured by spectrophotometric analysis (mean ± SD of three experiments).

B: PEITC-induced export of GSH from T72Ras and T72 cells to the culture medium (mean ± SD of three experiments).

C: Reversion of the PEITC-induced ROS by catalase (CAT). T72Ras cells were preincubated with 2000 U/ml CAT for 1 hr followed by 5 μM PEITC (P) for 1.5 hr.

D: Effect of catalase on PEITC-induced GSH depletion. GSH levels were determined after T72Ras cells were treated with catalase and PEITC as in **C**. Error bars, mean ± SD of four measurements.

E: Effect of NAC on PEITC-induced depletion of GSH. T72Ras cells were pretreated with 3 mM NAC for 1 hr, followed by 5 μM PEITC for 1 or 3 hr (mean ± SD of three experiments).

F: Reversion of PEITC-induced ROS accumulation by NAC. T72Ras cells were treated with 3 mM NAC for 1 hr, followed by 5 μM PEITC for 5 hr. A representative histogram (P+N indicates PEITC + NAC) and quantitative bar graph (mean ± SD of three experiments) are shown.

G: Reversion of PEITC-induced cell death by NAC. T72Ras cells were treated with 3 mM NAC for 1 hr, followed by 10 μM PEITC for 5 hr. Representative dot plots and quantitative bar graph (mean ± SD of three experiments) are shown.

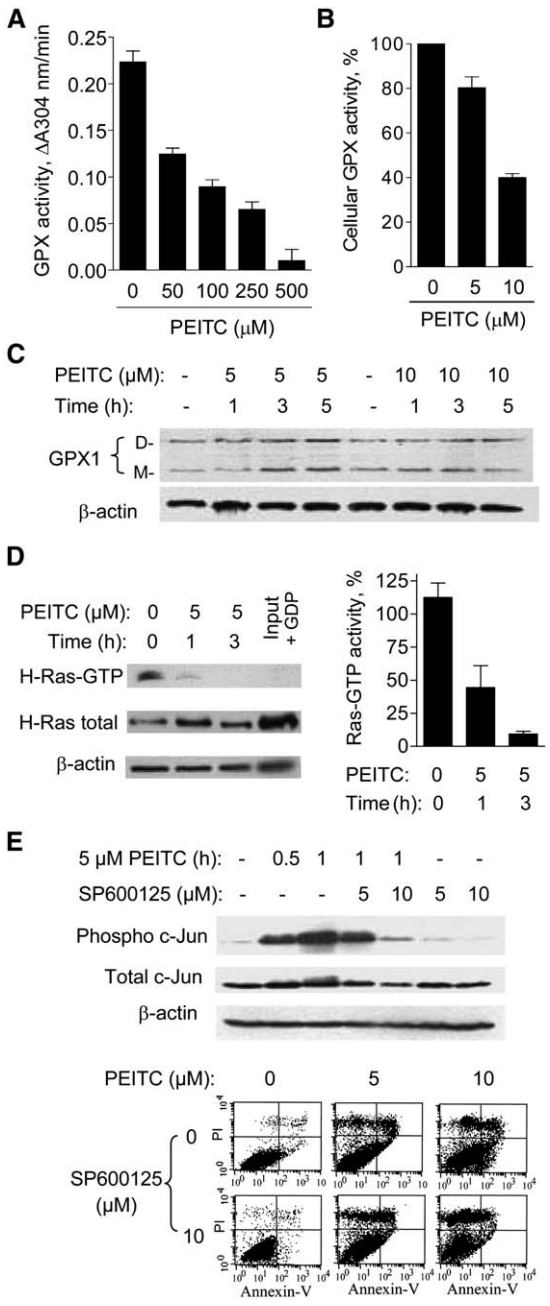

Figure 6. Effect of PEITC on GPX, H-RAS-GTP, and JNK activity

A: Dose-dependent inhibition of human GPX activity by PEITC in vitro (mean ± SD of three experiments).

B: Effect of PEITC on cellular GPX activity. T72Ras cells were incubated with 5–10 μM PEITC for 5 hr, and cellular protein extracts were assayed for GPX activity without addition of PEITC in vitro (mean ± SD of three experiments).

C: No decrease of GPX1 protein expression in T72Ras cells after PEITC treatment. GPX expression was determined by Western blot analysis. D, dimer; M, monomer.

D: Inhibition of RAS activation by PEITC. T72Ras cells were incubated with 5 μM PEITC for 1–3 hr, followed by RAS-GTP activity assay. The input/GDP lane is a negative control. The bar graph was calculated from the averaged band density of three experiments (mean ± SD).

E: Activation of JNK by PEITC and the effect of JNK inhibitor on PEITC-induced cell death. T72Ras cells were treated with the SP600125 for 1 hr followed by 5 μM PEITC. JNK activity was assayed by analysis of phospho c-Jun. Cell death was analyzed by flow cytometry after treatment with PEITC ± SP600125 (5 hr).

partially reversed the inactivation of H-RAS-GTP by PEITC (data not shown). Based on this observation, we then tested the effect of PEITC on another redox-sensitive molecule NF-κB, a transcription factor that responds to oxidative stress and promotes cell survival (Karin and Greten, 2005). Electrophoresis mobility shift assay showed that PEITC inhibited the basal and TNFα-stimulated NF-κB (p65/50) DNA binding activity (Figure S8). NAC decreased the PEITC-induced NF-κB inhibition. These data together suggest that the excessive ROS accumulation induced by PEITC may abrogate certain redox-sensitive molecules such as H-RAS and NF-κB, and thus impair cell survival signals. Furthermore, PEITC caused a rapid activation of the stress-activated protein kinase JNK in T72Ras cells, evidenced by a significant increase of c-Jun phosphorylation (Figure 6E). Interestingly, the JNK inhibitor SP600125 (10 μM) abolished PEITC-induced c-Jun phosphorylation (Figure 6E, upper panel) but did not significantly alter cell death (Figure 6E, lower panel), suggesting that JNK activation was likely a response to ROS stress, but not required to trigger cell death in T72Ras cells.

PEITC is effective in killing naturally occurring cancer cells and exhibits significant therapeutic activity in vivo

The ability of PEITC to cause severe ROS-mediated damage in the *Ras*-transformed cells prompted us to test its effectiveness in killing naturally occurring cancer cells. As shown in Figure 7A, PEITC was very effective in inhibiting proliferation of SKOV3 cells in both long-term MTT and colony formation assays, with the IC50 values of approximately 0.6 μM. About 95% of cell proliferating capacity was inhibited at 3 μM. Interestingly, the growth-inhibitory curve obtained by long-term MTT assay was comparable with colony formation assay (Figure 7A), suggesting that this MTT assay may be used to estimate the drug effect on proliferation of cells that can not readily form colonies, such as nontransformed cells. Flow cytometric analysis showed that a short-term incubation with PEITC (10 μM) caused acute cell death in more than half of the cells (Figures 7B and 7C). This cytotoxic effect was largely abrogated by NAC. Consistently, PEITC caused a substantial ROS increase, which was prevented by 3 mM NAC (Figure 7D).

We then further compared the effect of PEITC on two other ovarian cancer lines, A2008 (cisplatin-sensitive) and HEY (cisplatin-resistant) cells. As shown in Figures 7E–7G, A2008 cells were sensitive to PEITC, which exhibited significant cytotoxicity in a ROS-dependent manner (reversed by NAC; Figure 7E). Interestingly, although HEY cells were less sensitive to cisplatin, they were highly sensitive to PEITC (Figure 7H), suggesting that PEITC and cisplatin have different mechanisms of action. We also used a colony formation assay to examine the effect of PEITC on H1299 cells (lung cancer), and showed that this compound was similarly effective, with more than 90% of the colony forming capacity being abolished by 3 μM of PEITC (Figure S9).

The selectivity of PEITC against oncogenically transformed cells and its effectiveness in killing naturally occurring cancer cells in vitro led us to evaluate its activity in vivo. Nude mice were inoculated intraperitoneally (i.p.) with T72Ras cells, which grew tumor masses in peritoneal cavity and caused severe ascites (Figure 8A). Examination of the tumor sections revealed the histological morphology resembling that of human ovarian clear cell carcinoma (Figure 8B). Interestingly, the tumor also exhibited active angiogenesis with extensive newly formed blood vessels. Without drug treatment, the tumor-bearing mice started

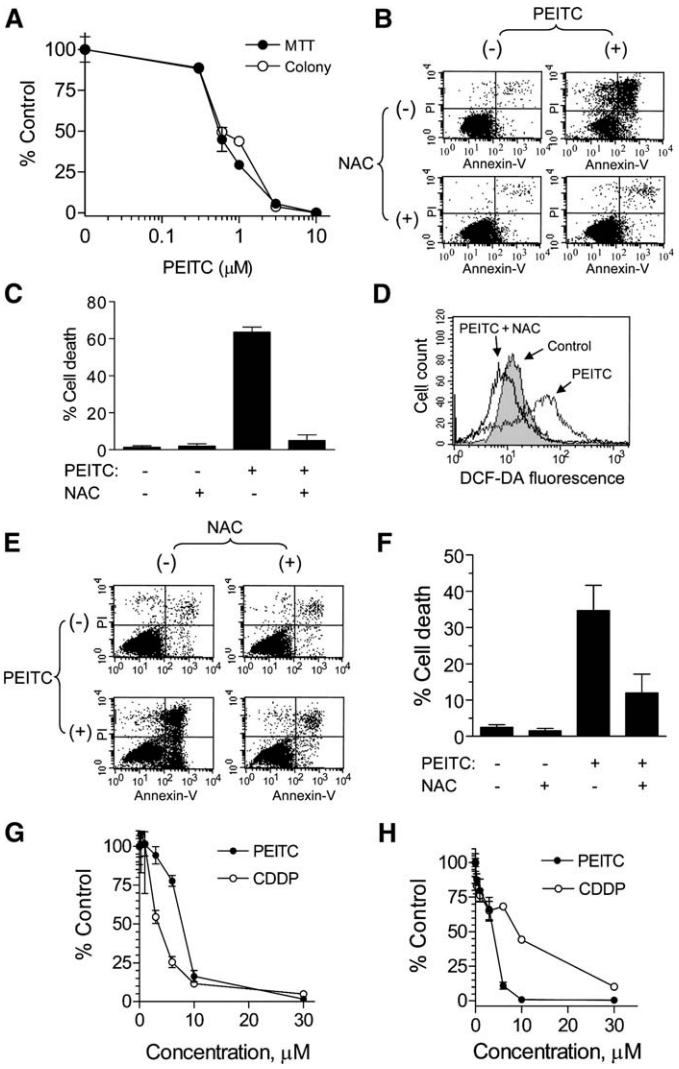

Figure 7. Cytotoxicity and ROS increase induced by PEITC in human ovarian cancer cells and the protective effect of NAC

A: Dose-dependent inhibition of cell proliferation and colony formation by PEITC in SKOV3 cells. Cell proliferation was measured by 10 day MTT assay and colony formation assay (mean ± SD of three experiments).
B: Acute cell death induced by PEITC. SKOV3 cells were preincubated with 3 mM NAC (1 hr) and then with 10 μM PEITC as indicated for 23 hr. Cell death was measured by flow cytometry.
C: Effect of NAC on PEITC-induced cell death in SKOV3 cells under the same conditions as in **B** (mean ± SD of three experiments).
D: Effect of PEITC and NAC on ROS levels in SKOV3 cells. Cells were incubated with 10 μM PEITC ± 3 mM NAC for 6 hr, and ROS were measured by flow cytometry using DCF-DA.
E: Induction of cell death by PEITC (10 μM, 24 hr) in A2008 cells in the presence or absence of 1 mM NAC. Cell death was detected by annexin-V/PI assay.
F: Quantitation of PEITC-induced cell death in A2008 cells in the presence and absence of NAC under the same conditions as in **E** (mean ± SD of three experiments).
G: Cytotoxicity of PEITC and CDDP in A2008 cells. Cells were incubated with each compound for 3 days, followed by MTT assay (mean ± SD of 3 measurements).
H: Comparison of cytotoxicity of PEITC and CDDP in ovarian cancer HEY cells. Cells were incubated with the indicated concentrations of each drug for 3 days followed by MTT assay (mean ± SD of three measurements).

to die about 18 days after tumor inoculation, and most of the animals died within 2 months. The median survival time for the untreated group (n = 20) was approximately 25 days (Figure 8C).

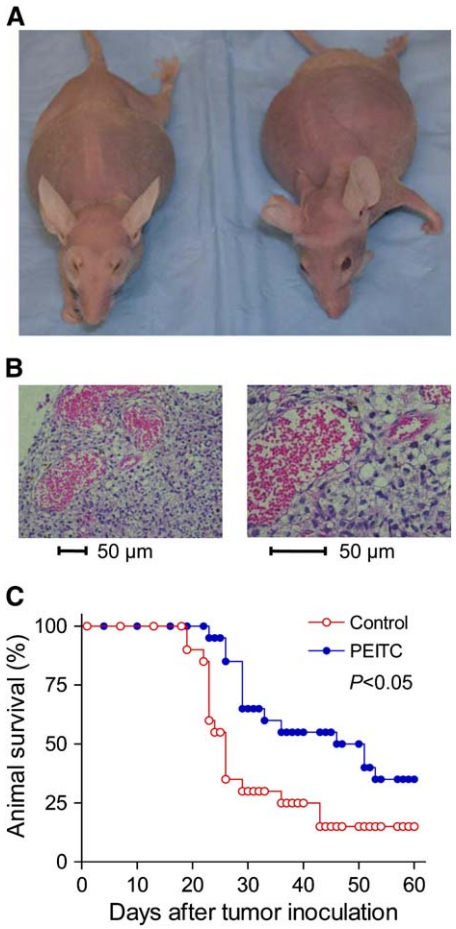

Figure 8. In vivo therapeutic activity of PEITC in mice bearing *Ras*-transformed ovarian cancer cells

Forty nude mice were inoculated with T72Ras cells (2×10^6 cells/mouse, i.p.) and randomly divided into two groups (20/group) for treatment with PEITC (50 mg/kg, i.p., daily, five times per week) or with control solvent as described in the Experimental Procedures.
A: Gross appearance of two mice with severe ascites.
B: Histological morphology of hematoxylin-eosin-stained tissue slices of the T72Ras tumor.
C: Comparison of animal survival of the PEITC-treated group and untreated group ($p < 0.05$).

In contrast, treatment with PEITC by i.p. injection (50 mg/kg, five times per week) significantly prolonged the animals' survival. The median survival time for the PEITC-treated animals was 48 days (n = 20), representing a 90% increase over that of the untreated group ($p < 0.05$; Figure 8C). No severe toxicity was observed, although some mice exhibited transient agitation at the time of drug injection. Some mice experienced a moderate level of reversible body weight loss.

Discussion

Increase of ROS stress in cancer cells has long been recognized and often viewed as an unfavorable event associated with carcinogenesis and cancer progression. However, recent studies showed that it is possible to use agents that promote cellular ROS accumulation to effectively kill cancer cells in vitro (Huang et al., 2000; Pelicano et al., 2003). Since oncogenes have been

shown to cause elevated ROS generation (Irani et al., 1997; Sattler et al., 2000; Vafa et al., 2002), the intrinsic oxidative stress associated with oncogenic transformation may render cancer cells highly dependent on their antioxidant systems to maintain redox balance and thus vulnerable to agents that impair antioxidant capacity. Inhibition of the antioxidant system in cancer cells would lead to a severe accumulation of ROS leading to cell death. In contrast, it is less likely to induce such severe ROS stress in normal cells, due to their low basal ROS output. This biochemical difference between normal and cancer cells may constitute a basis for modulating cellular ROS as a strategy to selectively kill cancer cells.

Using isogenic cell lines, here we showed that oncogenically transformed cells are more sensitive to ROS-mediated damage due to their high basal ROS generation, and that PEITC can be a selective anticancer agent based on this biological basis. Several lines of evidence support this conclusion. (1) Cells transformed with *H-Ras*^{V12} or *Bcr-Abl* exhibited a significant increase of ROS compared to their parental cells. (2) This intrinsic oxidative stress rendered them highly dependent on the GSH antioxidant system to maintain redox balance. Abolishing this system by PEITC through depletion of GSH and inhibition of GPX enzyme activity led to a preferential ROS increase in the transformed cells. (3) The severe accumulation of ROS in transformed cells caused oxidative damage to the mitochondria membranes and impaired the membrane integrity, leading to massive cell death. In contrast, PEITC caused only a modest increase of ROS insufficient to cause significant cell death in nontransformed cells. (4) The strong correlation between ROS accumulation and cell death induced by PEITC in T72Ras cells and the suppression of cytotoxicity by catalase or NAC suggest the critical role of ROS in PEITC-induced cell death. (5) The observations that BSO selectively killed transformed cells further support the role of GSH in maintaining redox balance and cancer cell survival. Based on these findings, it is likely that the therapeutic selectivity of PEITC is dependent on two important factors: the biological difference in redox regulation between the oncogenically transformed cells and normal cells, and the ability of PEITC to effectively abolish the GSH antioxidant system.

The elevated basal ROS in *Ras*-transformed cells seemed to include multiple reactive species detected by HEt (O_2^-) and DCF-DA (H_2O_2, NO, etc.). This increase of ROS is not surprising, since elevated generation of O_2^- can lead to an increase of other reactive species due to their intracellular conversion. The relatively low specificity of the chemical probes makes it difficult to accurately estimate the proportion of each reactive species in the cells. However, it is interesting to note that PEITC caused a further increase of reactive species that oxidized DCF-DA and DAF-FM but not HEt, suggesting that PEITC mainly induced accumulation of H_2O_2 (and other species such as NO) but not O_2^-.

PEITC has been shown to cause various degrees of ROS increase in hepatoma cells. A study in HepG2 cells showed only a minor role of ROS in PEITC-induced cell death (Rose et al., 2003), whereas a study in PLC/PRF/5 hepatoma cell line demonstrated that PEITC caused a significant ROS increase and induced cell death reversible by antioxidants (Wu et al., 2005). This variation may reflect different basal ROS levels in these cells. In our study, the degrees of ROS accumulation and cell death induced by PEITC were dependent on endogenous ROS generation. The high basal ROS in *Ras*- or *Bcr-Abl*-transformed cells seem responsible for their high sensitivity to PEITC. Because the transformed cells depend on GSH to counteract the active ROS output, abrogation of the GSH antioxidant system by PEITC would severely affect these cells, leading to oxidative damage. Our study showed that PEITC induced ROS accumulation by two mechanisms: depletion of GSH by promoting its export and inhibition of GPX enzyme activity, which together effectively disable the GSH antioxidant system.

Interestingly, incubation of cells with 5–10 μM PEITC led to a depletion of cellular GSH, which is in the mM range. The explanation for this stoichiometric discrepancy is that PEITC can be concentrated in the cells. A previous study showed that incubation of HL-60 cells with 5 μM [^{14}C]-PEITC for 3 hr resulted in an accumulation of PEITC at 0.5 nmole/10^6 cells (Xu and Thornalley, 2001), which is approximately in the mM range estimated based on the cell number and cell size. In our study, incubation of T72Ras cells with 5–10 μM PEITC for 2 hr led to intracellular concentrations of 0.25–0.59 mM. Furthermore, 0.5 mM PEITC was able to suppress more than 90% of GPX activity in the cell-free assay (Figure 6A). The ability of PEITC to rapidly deplete GSH and inhibit GPX, along with the active ROS production in cancer cells, may explain why this compound can cause a lethal accumulation of ROS in the malignant cells within several hours.

The PEITC-induced ROS accumulation in *Ras*-transformed cells seems to inactivate the redox-sensitive NF-κB and H-RAS. Both molecules contain cysteine residues that are essential for their functions but sensitive to oxidative modification due to the presence of thiol groups (Matthews et al., 1993; Mallis et al., 2001). Incubation of T72Ras cells with PEITC significantly inhibited the function of H-RAS to bind RAF-1 protein and suppressed the ability of NF-κB to bind its consensus DNA. Since this inactivation can be partially reversed by antioxidant NAC, it is likely that ROS play a role in mediating PEITC-induced inactivation of these two molecules. Oxidative inactivation of NF-κB has been observed in other experimental systems, and PEITC was recently shown to inhibit NF-κB in PC-3 cells (Khor et al., 2006). While activation of RAS by S-glutathionylation is known (Adachi et al., 2004), inactivation of RAS-GTP by ROS has not been well characterized. Because H-RAS and NF-κB play important roles in maintaining transformed phenotype and promoting cell survival, and NF-κB seems required for the survival of the *Ras*-transformed cells (Mayo et al., 1997), inactivation of these molecules by PEITC likely contributes to its anticancer activity.

The stress-activated protein kinase (SAPK)/JNK pathway plays an important role in cellular response to various stimuli, including oxidative stress. We observed that treatment of T72Ras cells with PEITC caused a rapid activation of JNK. This is consistent with the observations in other cancer cell lines (Hu et al., 2003; Xu et al., 2006). However, in PC-3 cells (prostate cancer) and HT-29 cells (colon cancer), activation of JNK is important for triggering apoptosis (Hu et al., 2003; Xu et al., 2006), whereas in *Ras*-transformed cells inhibition of JNK by SP600125 did not suppress PEITC-induced cell death. It is possible that the high level of ROS induced by PEITC in T72Ras cells caused lethal damage to mitochondria and other cellular components and did not require JNK activation to trigger cell death. Akt is another important molecule for cell survival. Recent studies suggest that PEITC is able to inhibit Akt activation, which may also contribute to its cytotoxic action (Khor et al., 2006; Satyan et al., 2006).

Cisplatin is a common drug for ovarian cancer treatment. Our study showed that PEITC has a superior selectivity compared to cisplatin. The ability to preferentially kill malignant cells is

a promising feature of PEITC. Interestingly, PEITC seems more toxic to leukemic cells than to normal lymphocytes (Xu and Thornalley, 2000). We demonstrated that PEITC preferentially killed oncogenically transformed cells by causing severe ROS accumulation and oxidative inactivation of H-RAS and NF-κB. This compound is also effective in naturally occurring cancer cells, including cisplatin-resistant cells. Furthermore, our animal study showed that PEITC has therapeutic activity in mice bearing *Ras*-transformed cells and prolongs median survival time by 90%. For a single agent, such in vivo activity seems promising. The effective concentrations of PEITC (0.5–10 μM) may be achievable in human. A pharmacokinetic study showed that an oral dose of 40 mg PEITC resulted in a plasma concentration of 1–2 μM (Liebes et al., 2001). Interestingly, a recent work showed that i.p. injection of PEITC (5 μmole, three times per week) retarded the growth of prostate cancer xenografts when given 1 day before tumor implantation (Khor et al., 2006). Although this dosage of PEITC had little effect on well-established tumor, combination of PEITC with curcumin was effective, suggesting that combination of PEITC with other agents may enhance anticancer activity.

In conclusion, our study suggests that the intrinsic oxidative stress in cancer cells associated with oncogenic transformation provides a basis for developing strategies to preferentially kill cancer cells through ROS-mediated mechanism, and compounds such as PEITC can be used to achieve such activity in vitro and in vivo. Importantly, cancer cells in advanced disease stage usually exhibit genetic instability and show significant increase in ROS generation due in part to the "vicious cycle" in which ROS induce mutations leading to further metabolic malfunction and more ROS generation (Pelicano et al., 2004). Such highly malignant cells are often resistant to conventional anticancer drugs. However, because these cells are under intrinsic ROS stress, using PEITC to preferentially kill such malignant cells warrants further testing in preclinical and clinical settings.

Experimental procedures

Reagents

PEITC, 3-(4,5 dimethylthiazol-2-yl)-2,5-diphenyltetrazolium (MTT), NAC, BSO, bovine catalase, and human GPX were purchased from Sigma-Aldrich (St. Louis, MO). Cisplatin (PLATINOL-AQ) was a product of Bristol-Myers Squibb (New York, NY). CM-H_2DCF-DA, HEt, NAO, carbony cyanide 3-chlorophenylhydrazone (CCCP), and Rho-123 were purchased from Invitrogen/Molecular Probes (Carlsbad, CA). SP600125 was acquired from EMD biosciences (Calbiochem, San Diego, CA). PEITC was dissolved in DMSO and freshly diluted in culture media before used. The final DMSO concentration was less than 0.1% (v/v).

Cell lines and cell culture

Both T72 (immortalized, nontumorigenic) and T72Ras (*H-Ras*^{V12}-transformed, tumorigenic) cell lines (Liu et al., 2004) were cultured in medium consisting of a 1:1 mix of MCDB105 and M199 medium (Sigma-Aldrich) with 15% fetal bovine serum and 10 ng/ml epidermal growth factor. TonB210 cells harboring a tetracycline-inducible *Bcr-Abl* expression vector (Klucher et al., 1998) were maintained in RPMI1640 medium with 10% FBS supplemented with IL-3 (supplied as 10% conditioned medium from Wehi3B cell culture). The IL3-dependent murine myeloid progenitor cell line DA1 and its stable *bcr-abl* transfectant line DA1-3b (Vereecque et al., 1999) were cultured in RPMI1640 medium. SKOV3, HEY, and H1299 were cultured in RPMI1640 medium with 10% FBS. A2008 cells were maintained in DMEM with 10% FBS.

Assays for cytotoxicity

Cell death was determined by flow cytometry after cells were double stained with annexin-V-FITC and propidium iodide (PI), using an assay kit from BD PharMingen (San Diego, CA) as described (Pelicano et al., 2003). To determine the drug effect on cell viability and long-term proliferation, we adapted the MTT assay by seeding cells in 24-well plates for drug treatment, followed by 10 day incubation. Cells were then incubated with MTT reagent for 4 hr, lysed with DMSO, and transferred to 96-well plate for quantitation by a plate reader. Since T72 cells could not form colonies, this 10 day MTT assay was used as an alternative assay for drug effect on long-term cell proliferation. Clonogenic assays were performed by seeding cells in 6-well plates, allowing adherence overnight, replacing the culture medium with 3 ml of fresh media containing PEITC at the specified concentrations, and incubating for 10 days. The cells were fixed and stained with 0.2% crystal violet (Sigma-Aldrich, St. Louis, MO), and colonies of >50 cells were counted.

Determination of cellular ROS

Cellular ROS contents were measured by incubating the control or drug-treated T72, T72Ras, or SKOV3 cells with 3 μM CM-H_2DCF-DA for 60 min, followed by flow cytometry using a FACSCalibur equipped with CellQuest Pro software. For TonB210 cells, 5 μM of CM-H_2DCF-DA was used in a 60 min labeling to obtained sufficient fluorescence signal. O_2^- was measured by flow cytometry using HEt (100 ng/ml) as described (Pelicano et al., 2003).

Analysis of cellular GSH and its export to the culture medium

A GSH assay kit (Cayman Chemical Co. Ann Arbor, MI) was used to measure total cellular glutathione. Cell extracts were prepared by sonication and deproteination using the conditions recommended by the manufacturer. Total GSH was detected by measuring the product of glutathionylated DTNB by UV spectrophotometer at 405 nm. The cellular GSH contents were calculated using the standard curve generated in parallel experiments. Cells number and median cell volume were quantified using a Coulter Z_2 particle count and size analyzer (Beckman Coulter, Inc., Fullerton, CA). To determine the effect of PEITC on GSH exported from cells to the culture medium, cells were plated in equal density and cultured for 24 hr. The medium was then replaced with serum-free medium with or without PEITC as indicated and incubated for 3 hr, and the culture medium was removed for GSH assay as described above.

Determination of oxidative damage to mitochondrial membranes

Mitochondrial membrane lipid peroxidation was detected by measuring the oxidation of cardiolipin, using NAO as a fluorescence dye (Nomura et al., 2000). After cells were incubated with or without PEITC, the samples were labeled with 50 nM NAO for 15 min and analyzed by flow cytometry. Changes in mitochondrial membrane potential were monitored by incubating cells with 1 μM Rho-123 for 1 hr, followed by flow cytometry. The decoupling agent CCCP was used as a positive control to induce membrane depolarization.

GPX enzyme activity assay

The GPX enzyme activity was assayed using continuous spectrophotometric rate determination as described (Wen et al., 2004). Human GPX (0.5 mU) purified from erythrocyte (Sigma-Aldrich) was premixed with or without PEITC for 10 min and added to a reaction mixture containing 2 mM GSH, 0.1 U glutathione reductase, and 0.2 mg/ml NADPH. Reaction was initiated by adding H_2O_2 (0.001%), and the kinetics of NADPH oxidation was monitored for 5 min at 340 nm. GPX activity (ΔA340 nm/min) was calculated by subtracting the slope of the reaction from that of spontaneous oxidation in the control sample. Cellular GPX activity was determined using an equal amount of protein extracts from control and PEITC-treated cells without further adding PEITC in the reactions.

Assay of H-RAS-GTP activity

RAS-GTP activity was determined based on its specific binding to the downstream effector RAF-1 as described (Marais et al., 1995). Protein extracts were prepared using the buffer provided in a RAS-GTP assay kit (Upstate Cell Signaling Solution, Charlottesville, VA). RAS-GTP activity in the cell extracts was detected by immunoprecipitation with 10 μg of RAF-1 binding peptide conjugated to agarose beads, followed by Western blot with 1:1000 anti-H-RAS antibody (Santa Cruz Biotechnology, Inc., Santa Cruz, CA). β-actin in whole-cell extracts was blotted as loading control. To verify the specificity of the GTP bound activity, the control extracts were preincubated with excess GDP to abolish the RAS-GTP ability to bind RAF-1

peptide, which yielded negative signal after immunoprecipitation with RAF-1-agarose.

Assay of in vivo antitumor activity of PEITC

Animal experiments were performed under federal guidelines and approved by the Institutional Animal Care and Use Committee (IACUC) of the University of Texas M.D. Anderson Cancer Center. Forty nude mice were inoculated with T72Ras cells (2×10^6 cells/mice, i.p.) and randomly divided into two groups (20 mice each). Three days after tumor inoculation, the treatment group received PEITC (50 mg/kg, i.p., five times per week). The control group received an equal volume of solvent control. The mice were monitored daily for signs of tumor growth, ascites, and body weight. Moribund animals were sacrificed as mandated by the IACUC protocol, and the time of death was recorded. Tumor tissues from representative mice were sectioned, embedded in paraffin, and stained with hematoxylin and eosin for histopathologic evaluation.

Statistical analysis

The statistical significance of the difference in cytotoxicity and ROS generation between transformed and nontransformed cells was evaluated using Student's t test. The statistical difference in animal survival curves between the control and PEITC-treated animal groups was analyzed using the log-rank test (two-tailed). These data analyses were performed using the Prism software (GraphPad, San Diego, CA). A p value of less than 0.05 was considered statistically significant.

Supplemental data

The Supplemental Data include nine supplemental figures and can be found with this article online at http://www.cancercell.org/cgi/content/full/10/3/241/DC1/.

Acknowledgments

The authors thank Tian-ai Wu, Yumin Hu, and Min Du for technical assistance. This work was supported in part by grants CA085563, CA100428, CA109041, and CA16672 from the National Institutes of Health. D.T. is a recipient of a scholarship from the Anandamahidol Foundation under the royal patronage of His Majesty the King of Thailand.

Received: January 22, 2006
Revised: June 3, 2006
Accepted: August 1, 2006
Published: September 11, 2006

References

Adachi, T., Pimentel, D.R., Heibeck, T., Hou, X., Lee, Y.J., Jiang, B., Ido, Y., and Cohen, R.A. (2004). S-glutathiolation of Ras mediates redox-sensitive signaling by angiotensin II in vascular smooth muscle cells. J. Biol. Chem. *279*, 29857–29862.

Balcerczyk, A., Soszynski, M., and Bartosz, G. (2005). On the specificity of 4-amino-5-methylamino-2′,7′-difluorofluorescein as a probe for nitric oxide. Free Radic. Biol. Med. *39*, 327–335.

Chen, Z., Trotman, L.C., Shaffer, D., Lin, H.K., Dotan, Z.A., Niki, M., Koutcher, J.A., Scher, H.I., Ludwig, T., Gerald, W., et al. (2005). Crucial role of p53-dependent cellular senescence in suppression of Pten-deficient tumorigenesis. Nature *436*, 725–730.

Couzin, J. (2002). Cancer drugs Smart weapons prove tough to design. Science *298*, 522–525.

Deneke, S.M. (2000). Thiol-based antioxidants. Curr. Top. Cell. Regul. *36*, 151–180.

Frantz, S. (2005). Drug discovery: Playing dirty. Nature *437*, 942–943.

Hampton, M.B., Stamenkovic, I., and Winterbourn, C.C. (2002). Interaction with substrate sensitises caspase-3 to inactivation by hydrogen peroxide. FEBS Lett. *517*, 229–232.

Hockenbery, D.M., Oltvai, Z.N., Yin, X.M., Milliman, C.L., and Korsmeyer, S.J. (1993). Bcl-2 functions in an antioxidant pathway to prevent apoptosis. Cell *75*, 241–251.

Hu, R., Kim, B.R., Chen, C., Hebbar, V., and Kong, A.N. (2003). The roles of JNK and apoptotic signaling pathways in PEITC-mediated responses in human HT-29 colon adenocarcinoma cells. Carcinogenesis *24*, 1361–1367.

Hu, Y., Rosen, D.G., Zhou, Y., Feng, L., Yang, G., Liu, J., and Huang, P. (2005). Mitochondrial manganese-superoxide dismutase expression in ovarian cancer: Role in cell proliferation and response to oxidative stress. J. Biol. Chem. *280*, 39485–39492.

Huang, P., Feng, L., Oldham, E.A., Keating, M.J., and Plunkett, W. (2000). Superoxide dismutase as a target for the selective killing of cancer cells. Nature *407*, 390–395.

Irani, K., Xia, Y., Zweier, J.L., Sollott, S.J., Der, C.J., Fearon, E.R., Sundaresan, M., Finkel, T., and Goldschmidt-Clermont, P.J. (1997). Mitogenic signaling mediated by oxidants in Ras-transformed fibroblasts. Science *275*, 1649–1652.

Karin, M., and Greten, F.R. (2005). NF-κB: Linking inflammation and immunity to cancer development and progression. Nat. Rev. Immunol. *5*, 749–759.

Khor, T.O., Keum, Y.S., Lin, W., Kim, J.H., Hu, R., Shen, G., Xu, C., Gopalakrishnan, A., Reddy, B., and Zheng, X. (2006). Combined inhibitory effects of curcumin and phenethyl isothiocyanate on the growth of human PC-3 prostate xenografts in immunodeficient mice. Cancer Res. *66*, 613–621.

Klucher, K.M., Lopez, D.V., and Daley, G.Q. (1998). Secondary mutation maintains the transformed state in BaF3 cells with inducible BCR/ABL expression. Blood *91*, 3927–3934.

Liebes, L., Conaway, C.C., Hochster, H., Mendoza, S., Hecht, S.S., Crowell, J., and Chung, F.L. (2001). High-performance liquid chromatography-based determination of total isothiocyanate levels in human plasma: Application to studies with 2-phenethyl isothiocyanate. Anal. Biochem. *291*, 279–289.

Liu, J., Yang, G., Thompson-Lanza, J.A., Glassman, A., Hayes, K., Patterson, A., Marquez, R.T., Auersperg, N., Yu, Y., and Hahn, W.C. (2004). A genetically defined model for human ovarian cancer. Cancer Res. *64*, 1655–1663.

Mallis, R.J., Buss, J.E., and Thomas, J.A. (2001). Oxidative modification of H-ras: S-thiolation and S-nitrosylation of reactive cysteines. Biochem. J. *355*, 145–153.

Marais, R., Light, Y., Paterson, H.F., and Marshall, C.J. (1995). Ras recruits Raf-1 to the plasma membrane for activation by tyrosine phosphorylation. EMBO J. *14*, 3136–3145.

Matthews, J.R., Kaszudska, W., Turcatti, G., Wells, T.N.C., and Hay, R.T. (1993). Role of cysteine 62 in DNA recognition by the P50 subunit of NF-κB. Nucleic Acids Res. *21*, 1727–1734.

Mayo, M.W., Wang, C.Y., Cogswell, P.C., Rogers-Graham, K.S., Lowe, S.W., Der, C.J., and Baldwin, A.S., Jr. (1997). Requirement of NF-κB activation to suppress p53-independent apoptosis induced by oncogenic Ras. Science *278*, 1812–1815.

Nomura, K., Imai, H., Koumura, T., Kobayashi, T., and Nakagawa, Y. (2000). Mitochondrial phospholipid hydroperoxide glutathione peroxidase inhibits the release of cytochrome c from mitochondria by suppressing the peroxidation of cardiolipin in hypoglycaemia-induced apoptosis. Biochem. J. *351*, 183–193.

Pelicano, H., Feng, L., Zhou, Y., Carew, J.S., Hileman, E.O., Plunkett, W., Keating, M.J., and Huang, P. (2003). Inhibition of mitochondrial respiration: A novel strategy to enhance drug-induced apoptosis in human leukemia cells by a reactive oxygen species-mediated mechanism. J. Biol. Chem. *278*, 37832–37839.

Pelicano, H., Carney, D., and Huang, P. (2004). ROS stress in cancer cells and therapeutic implications. Drug Resist. Updat. *7*, 97–110.

Radisky, D.C., Levy, D.D., Littlepage, L.E., Liu, H., Nelson, C.M., Fata, J.E., Leake, D., Godden, E.L., Albertson, D.G., Nieto, M.A., et al. (2005). Rac1b and reactive oxygen species mediate MMP-3-induced EMT and genomic instability. Nature *436*, 123–127.

Ren, R. (2005). Mechanisms of BCR-ABL in the pathogenesis of chronic myelogenous leukaemia. Nat. Rev. Cancer *5*, 172–183.

Rose, P., Whiteman, M., Huang, S.H., Halliwell, B., and Ong, C.N. (2003). Beta-Phenylethyl isothiocyanate-mediated apoptosis in hepatoma HepG2 cells. Cell. Mol. Life Sci. *60*, 1489–1503.

Sattler, M., Verma, S., Shrikhande, G., Byrne, C.H., Pride, Y.B., Winkler, T., Greenfield, E.A., Salgia, R., and Griffin, J.D. (2000). The BCR/ABL tyrosine kinase induces production of reactive oxygen species in hematopoietic cells. J. Biol. Chem. *275*, 24273–24278.

Satyan, K.S., Swamy, N., Dizon, D.S., Singh, R., Granai, C.O., and Brard, L. (2006). Phenethyl isothiocyanate (PEITC) inhibits growth of ovarian cancer cells by inducing apoptosis: Role of caspase and MAPK activation. Gynecol Oncol. Published online April 17, 2006. 10.1016/j.ygyno.2006.03.002.

Sureda, F.X., Escubedo, E., Gabriel, C., Comas, J., Camarasa, J., and Camins, A. (1997). Mitochondrial membrane potential measurement in rat cerebellar neurons by flow cytometry. Cytometry *28*, 74–80.

Swartz, H.M., and Gutierrez, P.L. (1977). Free radical increases in cancer: Evidence that there is not a real increase. Science *198*, 936–938.

Szatrowski, T.P., and Nathan, C.F. (1991). Production of large amounts of hydrogen peroxide by human tumor cells. Cancer Res. *51*, 794–798.

Vafa, O., Wade, M., Kern, S., Beeche, M., Pandita, T.K., Hampton, G.M., and Wahl, G.M. (2002). c-Myc can induce DNA damage, increase reactive oxygen species, and mitigate p53 function: A mechanism for oncogene-induced genetic instability. Mol. Cell *9*, 1031–1044.

Vereecque, R., Buffenoir, G., Gonzalez, R., Preudhomme, C., Fenaux, P., and Quesnel, B. (1999). A new murine aggressive leukemic model. Leuk. Res. *23*, 415–416.

Wen, J.J., Vyatkina, G., and Garg, N. (2004). Oxidative damage during chagasic cardiomyopathy development: Role of mitochondrial oxidant release and inefficient antioxidant defense. Free Radic. Biol. Med. *37*, 1821–1833.

Wu, S.J., Ng, L.T., and Lin, C.C. (2005). Effects of antioxidants and caspase-3 inhibitor on the phenylethyl isothiocyanate-induced apoptotic signaling pathways in human PLC/PRF/5 cells. Eur. J. Pharmacol. *518*, 96–106.

Xu, K., and Thornalley, P.J. (2000). Studies on the mechanism of the inhibition of human leukaemia cell growth by dietary isothiocyanates and their cysteine adducts *in vitro*. Biochem. Pharmacol. *60*, 221–231.

Xu, K., and Thornalley, P.J. (2001). Involvement of glutathione metabolism in the cytotoxicity of the phenethyl isothiocyanate and its cysteine conjugate to human leukemia cells in vitro. Biochem. Pharmacol. *61*, 165–177.

Xu, C., Shen, G., Yuan, X., Kim, J.H., Gopalkrishnan, A., Keum, Y.S., Nair, S., and Kong, A.N. (2006). ERK and JNK signaling pathways are involved in the regulation of activator protein 1 and cell death elicited by three isothiocyanates in human prostate cancer PC-3 cells. Carcinogenesis *27*, 437–445.

Yu, R., Mandlekar, S., Harvey, K.J., Ucker, D.S., and Kong, A.N. (1998). Chemopreventive isothiocyanates induce apoptosis and caspase-3-like activity. Cancer Res. *58*, 402–408.

Zhang, Y., Tang, L., and Gonzalez, V. (2003). Selected isothiocyanates rapidly induce growth inhibition of cancer cells. Mol. Cancer Ther. *2*, 1045–1052.

Zhao, H., Kalivendi, S., Zhang, H., Joseph, J., Nithipatikom, K., Vasquez-Vivar, J., and Kalyanaraman, B. (2003). Superoxide reacts with hydroethidine but forms a fluorescence product that is distinctly different from ethidium: Potential implications in intracellular fluorescence detection of superoxide. Free Radic. Biol. Med. *34*, 1359–1368.

Zhou, Y., Hileman, E.O., Plunkett, W., Keating, M.J., and Huang, P. (2003). Free radical stress in chronic lymphocytic leukemia cells and its role in cellular sensitivity to ROS-generating anticancer agents. Blood *101*, 4098–4104.